**Naval Research Laboratory**
Washington, DC 20375-5320

NRL/MR/7140--97-7905

# Bottom Backscattering Measured Off the South Carolina Coast During Littoral Warfare Advanced Development Focused Technology Experiment 96-2

RAYMOND J. SOUKUP
PETER M. OGDEN

*Acoustic Systems Branch*
*Acoustics Division*



April 28, 1997

Approved for public release; distribution is unlimited

# REPORT DOCUMENTATION PAGE

*Form Approved*
*OMB No. 0704-0188*



| 1. AGENCY USE ONLY (*Leave Blank*) | 2. REPORT DATE | 3. REPORT TYPE AND DATES COVERED |
|---|---|---|
| | April 28, 1997 | Interim Report |

**4. TITLE AND SUBTITLE**

Bottom Backscattering Measured Off the South Carolina Coast During Littoral Advanced Development Focused Technology Experiment 96-2

**5. FUNDING NUMBERS**

PE - 06037447N

**6. AUTHOR(S)**

Raymond J. Soukup and Peter M. Ogden

**7. PERFORMING ORGANIZATION NAME(S) AND ADDRESS(ES)**

Naval Research Laboratory
Washington, DC 20375-5320

**8. PERFORMING ORGANIZATION REPORT NUMBER**

NRL/MR/7140--97-7905

**9. SPONSORING/MONITORING AGENCY NAME(S) AND ADDRESS(ES)**

Office of Naval Research, Code 32
Arlington, VA 22217-5000

**10. SPONSORING/MONITORING AGENCY REPORT NUMBER**

**11. SUPPLEMENTARY NOTES**

**12a. DISTRIBUTION/AVAILABILITY STATEMENT**

Approved for public release; distribution unlimited.

**12b. DISTRIBUTION CODE**

A

**13. ABSTRACT** (*Maximum 200 words*)

Measurements of ocean bottom backscattering were performed in a shallow water environment off the coast of South Carolina as part of the Littoral Warfare Advanced Development (LWAD) Focused Technology Experiment 96-2 (FTE 96-2). Scattering strengths were obtained at 2, 2.5, 3 and 3.5 kHz as a function of grazing angle. The site dependence arising from the presence or absence of a sandy sediment layer was investigated; the results were consistent with observations of sediment thickness on a seismic track.

Scattering strengths in the absence of sediment were on the order of −13 dB and relatively frequency independent, while scattering strengths in the presence of the sediment layer were 15-20 dB lower and showed some frequency dependence, suggesting the influence of attenuation effects within the sediment. The grazing angle dependence could be fit adequately by assuming a dependence of scattering strength on the sine of the grazing angle.

**14. SUBJECT TERMS**

Bottom scattering
Sediment wedge
Reverberation
Active sonar
Underwater acoustics

**15. NUMBER OF PAGES**

17

**16. PRICE CODE**

| 17. SECURITY CLASSIFICATION OF REPORT | 18. SECURITY CLASSIFICATION OF THIS PAGE | 19. SECURITY CLASSIFICATION OF ABSTRACT | 20. LIMITATION OF ABSTRACT |
|---|---|---|---|
| UNCLASSIFIED | UNCLASSIFIED | UNCLASSIFIED | UL |

## CONTENTS

# BOTTOM BACKSCATTERING MEASURED OFF THE SOUTH CAROLINA COAST DURING LITTORAL WARFARE ADVANCED DEVELOPMENT FOCUSED TECHNOLOGY EXPERIMENT 96-2

## 1 Introduction

As a source of strong and persistent low-Doppler reverberation and clutter, acoustic interaction with the ocean bottom must be understood and quantified, especially in littoral-water environments where it can be the limiting factor in active sonar performance. Bottom scattering strength (BSS) is a standard input to active system performance prediction models, providing a characterization of bottom interaction for sound paths that backscatter from the ocean bottom and return to the receiver. Analysis of the site dependence, grazing-angle dependence, and frequency dependence of BSS provide physical insight into bottom scattering mechanisms. The bottom interaction problem involves several physical processes, all of which may contribute to the measured scattering strength: scattering from the water/sediment interface, scattering in the sediment volume itself, or scattering from the basement or a subsurface layer with a significant impedance mismatch. The frequency and grazing-angle dependence can reflect an enhancement of one mechanism over another, and given the variability of the littoral environment in sediment thickness, composition, and frequency-dependent attenuation, correct physical interpretation of bottom scattering strengths requires significant knowledge of the geoacoustic properties and structure of the subbottom.

Bottom backscattering results in the 2 to 3.5 kHz frequency regime have been summarized in a survey article by McCammon [1]. Among other conclusions, McCammon cites frequency dependence and grazing angle dependence as unresolved issues. Regarding grazing angle dependence, McCammon notes that scattering strengths at these frequencies tend to follow an omnidirectional scattering model (for which scattering strength is proportional to $\sin\theta$, where $\theta$ is the grazing angle) rather than Lambert's law (scattering strength proportional to $\sin^2\theta$ for the case where the incident and reflected grazing angles are the same), which is more common at lower frequencies.

The Critical Sea Test (CST) Program has also been investigating the causes of bottom backscattering, primarily in the frequency range from 100 to 1500 Hz. In a summary white paper, Holland *et al.* [2] note that it is important to investigate backscattering strengths over a wide range of grazing angles, because it is possible for different scattering mechanisms to be dominant at different grazing angles. For this reason it is important to try to measure directly lower grazing-angle results rather than using higher-angle results to extrapolate to lower angles of tactical interest.

Bottom scattering strength can be calculated by solving the sonar equation in the following form:

$$\mathrm{BSS} = \mathrm{RL} - \mathrm{SL} + \mathrm{TL}_s + \mathrm{TL}_r - 10\log \mathrm{A} \qquad (1)$$

Manuscript approved March 20, 1997

where BSS is the scattering strength in dB, RL is the measured reverberation level in dB *re* $(1\mu\text{Pa})^2/\text{Hz}$, SL is the source level in dB *re* $(1\mu\text{Pa})^2/\text{Hz}$ at 1 m, $\text{TL}_s$ is the transmission loss from the source to the ensonified patch on the bottom in dB, $\text{TL}_r$ is the transmission loss from the ensonified patch on the bottom to the receiver in dB, and A is the area of the ensonified patch in square meters.

In this report, BSS results obtained from a monostatic system in a littoral environment off the coast of South Carolina are presented. A map of the experiment site is shown in Fig. 1. The measurements were conducted in support of the Littoral Warfare Advanced Development (LWAD) Project, which provides proof of concept experiments for littoral undersea warfare science and technology projects. For the Focused Technology Experiment 96-2 (FTE 96-2) in August 1996, bottom backscattering measurements were made over a wide range of grazing angles of several sites close to the continental shelf. Data were obtained at four frequencies (2, 2.5, 3 and 3.5 kHz) and three sites (water depths = 120, 230, and 310 m), typically covering grazing angles of 10 to 50 degrees. The locations of the runs are shown in Fig. 2.

The FTE 96-2 bottom backscattering analysis centered on the relationship between the geoacoustic characteristics and the bottom scattering strengths. Scattering strengths were obtained from two types of sites: a site (site B) with a significant sandy sediment thickness that allowed for attenuation effects to be present, and two sites (sites Q and C) where sediment was negligible and the underlying limestone acted as the scatterer. In this report, the results are summarized in the form of an empirical model for grazing angle dependence and compared with the scattering levels described by McCammon [1].

## 2 Experiment geometry and data analysis

The bottom scattering tests were conducted from the research vessel SEAWARD EXPLORER during FTE 96-2. A schematic diagram of the geometry is shown in Fig. 3. A vertical line array (VLA) and a source were deployed on a single cable, with the source located 3 m below the center of the VLA. This resulted in a nearly monostatic measurement geometry.

The source was an omnidirectional spherical transducer (USRD F80) that gave root-mean-square source levels ranging from 181 dB at 2 kHz to 187 dB at 3.5 kHz. At each site, the source was placed successively at three different depths (a subset of 35, 60, 65, 85 and 105 m) and a set of pings was transmitted at each depth. The waveforms were 50 millisecond CW's at frequencies of 2.0, 2.5, 3.0, and 3.5 kHz. Sets of 12 to 15 identical pings were transmitted at each frequency, with individual pings separated by 10 s. A typical source raytrace and sound speed profile are shown in Fig. 4.

The bottom reverberation from the 50 millisecond pulses was received on a 9-hydrophone aperture of the VLA. The hydrophones were spaced at 21 cm, which corresponded to a half-wavelength spacing of 3570 Hz. Ten beams with cosine-spaced main response axes were formed from the aperture, with most the returns of interest coming from three downward-looking beams closest to broadside. For FTE 96-2, the maximum horizontal range used for a scatterer-to-receiver path was approximately 1.5 km.

After beamforming, power spectra were obtained using 50 millisecond FFT's with 50 percent overlap. A frequency band representing the total energy about the zero-Doppler

peak was selected and a time series was created for each ping including only the energy in this band. The direct arrivals for the pings were then temporally aligned and the various pings were averaged to produced a single reverberation curve for each beam and frequency bin. Integration over the roughly zero-Doppler spectral peak produced the total returned power as a function of time and beam. By calculating geometric spreading loss along each ray path, the transmission loss terms to and from the scattering patch were obtained. Finally, the computed beam pattern and raytrace were used to calculate the scattering patch area. From these inputs, BSS was calculated using Eq. 1 as a function of beam, frequency and grazing angle. Additional details about the processing scheme are given by Ogden and Erskine [3]. The standard deviations due to ping-to-ping variability were $\pm$ 2 to 3 dB, which is comparable to the expected experimental uncertainty of about $\pm$ 4 dB.

# 3 Bottom scattering results

## 3.1 Site and grazing angle dependence

In the FTE 96-2 test area, the ocean bottom east of the shelf break features a sedimentary wedge of calcareous sand [4]. Gulf Stream activity scours the bottom, limiting the water depth at which this sediment layer is observed. In Fig. 5, a seismic trace from a southeast-northwest track ending in the vicinity of site B shows that the underlying limestone is exposed for water depths greater than 170 m, based on the two-way travel time and a 1530 m/s sound speed. (The FTE 96-2 Environmental Assessment cites a different limiting water depth of 400 m [5]. The 170 m value is consistent with bottom scattering results shown below). Sediment layer thickness at the end of the track is 25 m, assuming a 1700 m/s compressional sound speed in the sediment.

Bottom scattering strengths at 2000 and 3500 Hz for site B are shown in Fig. 6 and 7. The two figures exhibit different ranges of grazing angles obtained from two deployments 24 minutes apart with source depths of 60 and 35 m respectively. For this experimental geometry, the grazing angles for the source-to-scatterer and scatterer-to-receiver are similar, so only one angle needs to be considered in the analysis. A reference curve showing Lambert's law with a coefficient of -27 dB is provided. This curve represents the standard input to Navy performance models, with the selection of the -27 dB value originating in the work of MacKenzie [6]. Data points above the reference curve represent the potential for underestimating the reverberation background and obtaining errors in system performance prediction via the standard model. For Figures 6 and 7, the majority of data points represent stronger scattering than the assumption by the standard model.

While the scattering results of Fig. 6 show a Lambert-like dependence on grazing angle, the scattering results of Fig. 7 do not. As shown in section 3.3, they can be fit much better assuming a dependence on the sine of the grazing angle rather than the square of the sine of the grazing angle. The beams numbered 2, 3, and 4 in Figs. 6 and 7 correspond to main response axis directions of 33.8, 19.5 and 6.4 degrees relative to broadside. There is no obvious dependence on beam. No obvious explanation is evident for the differences seen in Figs. 6 and 7 for the two measurement depths. At the other sites, there were no significant discrepancies among the results for the different source depths. Site B is significantly shallower than sites Q and C, however, making it more subject to small changes

in the geometry and environment.

Results for sites Q and C, which are outside the sediment wedge area, are shown in Figs. 8 and 9. Here the levels are significantly higher than those of the sediment wedge area. The results at these two sites are consistent, as they both represent scattering from the limestone. The scattering is flatter with respect to grazing angle than the reference curve and exhibits a similar angular dependence to the site B results in Figure 7. Another similarity is the lack of dependence on beam.

### 3.2 Frequency dependence

Attenuation values of at least 1 dB/m are expected in the calcerous sand wedge at 2 kHz and above [7,8]. As a result, there is probably no interaction with the underlying limestone at site B, assuming that the sediment thickness is on the order of the 25 m value cited above. Therefore, the scattering results at site B represent scattering within the sediment volume or with the water/sediment interface. The observed decrease of scattering strength at site B with increasing frequency is an indicator that the sediment volume is involved in the scattering, as attenuation increases with increasing frequency. Figures 10 and 11 give the results for four different frequencies in sites B and C with the 35 m source depth As an initial estimate it might be assumed that the linear dependence of attenuation on frequency found in many data sets would produce such a linear dependence in the scattering strength values at site B. The reason for the departure from the simple linear model for the measurements at 3500 Hz for site B is not known. Site C (Fig. 11) results reflect the lack of sediment, as there is presumably negligible penetration into the bottom. Therefore there is no frequency dependence due to attenuation, but rather values which are very close. There is a slight increase in bottom scattering strength with frequency that may or may not be significant. An explanation may lie in the roughness properties of the bottom, which are not well-known.

### 3.3 Model fits to scattering results

The above results, with the exception of the low-grazing angle data from site B, are consistent with scattering proportional to the sine of the grazing angle. On a dB scale, this is

$$BSS = 10\log(\sin\theta) + \mu \tag{2}$$

Since some performance models require a Lambert's law model, the model

$$BSS = 10\log(\sin^2\theta) + \mu \tag{3}$$

is also considered. Except for the low grazing angle results of site B (Fig. 6), this is a poor fit to the data. For the site B low grazing angles the latter model is somewhat better. Table 1 gives the value of $\mu$ for both models. The two entries for site B are the values obtained at the 35 and 60 m source depths respectively, the latter representing a lower grazing angle sample.

The values of Table 1 are comparable to historical data. McCammon gives an average $\mu$ value of $-18.7 \pm 8.6$ dB assuming $\sin\theta$ dependence for a group of data sets from rock, coarse sand, and shell bottoms. The site C and Q values for the $\sin\theta$ column of Table 1 all lie above

Table 1: Values of $\mu$ for LWAD FTE 96-2

| Site | Bottom Type | Grazing Angles (deg) | Frequency (Hz) | $\sin\theta$ model ($\mu$) | $\sin^2\theta$ model ($\mu$) |
|---|---|---|---|---|---|
| C | Limestone | 15-55 | 2000 | -15.6 | -11.6* |
| | | | 2500 | -14.4 | -10.4* |
| | | | 3000 | -13.7 | -9.6* |
| | | | 3500 | -13.4 | -9.3* |
| Q | Limestone | 15-55 | 2000 | -16.0 | -11.5* |
| | | | 2500 | -14.8 | -10.6* |
| | | | 3000 | -13.2 | -9.0* |
| | | | 3500 | -13.2 | -8.9* |
| B | Sand over limestone | 12-28/8-20 | 2000 | -24.9/-27.9 | -19.5/-20.9 |
| | | | 2500 | -23.9/-25.8 | -18.6/-18.8 |
| | | | 3000 | -26.7/-28.4 | -21.2/-21.3 |
| | | | 3500 | -31.9/-30.8 | -26.2/-23.8 |

Note: The fits with an asterisk represent significant lack of fit and are not recommended.

McCammon's average value. This is plausible as the data sets described in the reference are mostly of the sand variety and the limestone bottom at these sites should produce higher scattering strengths. The data for rock given by McCammon are limited, but has similar levels to this data.

A similar comparison can be made for the site B values. McCammon gives $-27.5 \pm 6.8$ dB as an average $\mu$ value assuming $\sin\theta$ for fine sand and silt bottoms. Some of the data sets included in this average value are at frequencies less than 2 kHz with lower $\mu$ values. The $\mu$ values obtained for FTE 96-2 are more consistent with the higher frequency measurements given by McCammon. In any case all the values fall within McCammon's interval.

## 4 Summary

During LWAD FTE 96-2 bottom backscattering strengths were measured at three sites within the test area. The water depths at these sites ranged from 120 m at site B to 310 m at site C. At sites Q and C, the bottom consisted of solid limestone with very little sediment cover, while at site B there was a sand layer approximately 25 m deep overlying the limestone. As expected, the bottom scattering strenghts reflected this difference in bottom character. At sites Q and C, the scattering strengths were very high, showed little frequency dependence, and tended to follow a $\sin\theta$ grazing angle dependence. At site B, the presence of the sand caused the acoustic energy to be attenuated before it could scatter off the limestone bottom. The resulting scattering strengths, while still higher than the Navy standard Mackenzie levels, are substantially lower than the levels from sites Q and C. In addition, there is evidence of a frequency dependence in the scattering results from site B: the 3500 Hz levels are as much as 8 dB lower than the 2000 Hz levels for one of the site B deployments. However, not all of the site B results support this conclusion, so the issue of

frequency dependence due to the sand layer is not resolved.

The LWAD FTE 96-2 measurements provided an opportunity to support analysis of scattering strength results with seismic measurements of sediment thickness. This provided a plausible explanation for site and frequency dependence. To assess the environment as a whole, more measurements would need to be made at different frequencies and other grazing angles, in conjunction with measurement of the sediment layer thickness. More knowledge of the properties of the sediment and limestone would provide the opportunity to fit the scattering strength data with a physics-based model. Based on the measurements obtained here, one can arrive at a consistent empirical model that represents the first-order bottom scattering characteristics of the FTE 96-2 experimental area.

## 5 Acknowledgments

This work was sponsored by the Office of Naval Research Littoral Warfare Advanced Development Project, CDR M. N. Shipley, Program Manager. We thank Dennis Dundore of the Naval Research Laboratory and Jerome Richardson and Elisabeth Kim of Planning Systems Incorporated for assistance with the data processing.

## 6 References

1. D.F. McCammon, "Low Grazing Angle Bottom Scattering Strength: Survey of Unclassified Measurements and Models and Recommendations for LFA Use (U)," JUA(USN) **43**[1] (Secret), January 1993 (Unclassified), 33-47.

2. C.W. Holland, P.M. Ogden, M.T. Sundvik, and R. Dicus, "Critical Sea Test Bottom Interaction Overview," Critical Sea Test White Paper SPAWAR CST/LLFA-WP-EVA-46, September 1996.

3. P.M. Ogden and F.T. Erskine, "Surface scattering measurements using broadband explosive charges in the Critical Sea Test experiments," J. Acoust. Soc. Am. **95**, 746-761 (1994).

4. C.K. Paull and W.P. Dillon, "Structure, Stratigraphy, and Geologic History of Florida-Hatteras Shelf and inner Blake Plateau", AAPG Bull., **64**, p. 339-358.

5. P.J. Bucca, J.K. Fulford, G.A. Kerr and R.W. Nero, "Appendix O: Environmental Assessment for the Littoral Warfare Advanced Development Focused Technology Experiment (FTE 96-2)", Naval Research Laboratory, Stennis Space Center, MS, August 7, 1996.

6. K.V. Mackenzie, "Bottom Reverberation for 530 and 1030 cps Sound in Deep Water," J. Acoust. Soc. Am **33**, 1498-1504 (1961).

7. C.S. Clay and H. Medwin, *Acoustical Oceanography: Principles and Applications*, John Wiley and Sons, New York (1977).

8. Dr. Steve Snyder, North Carolina State University, private communication

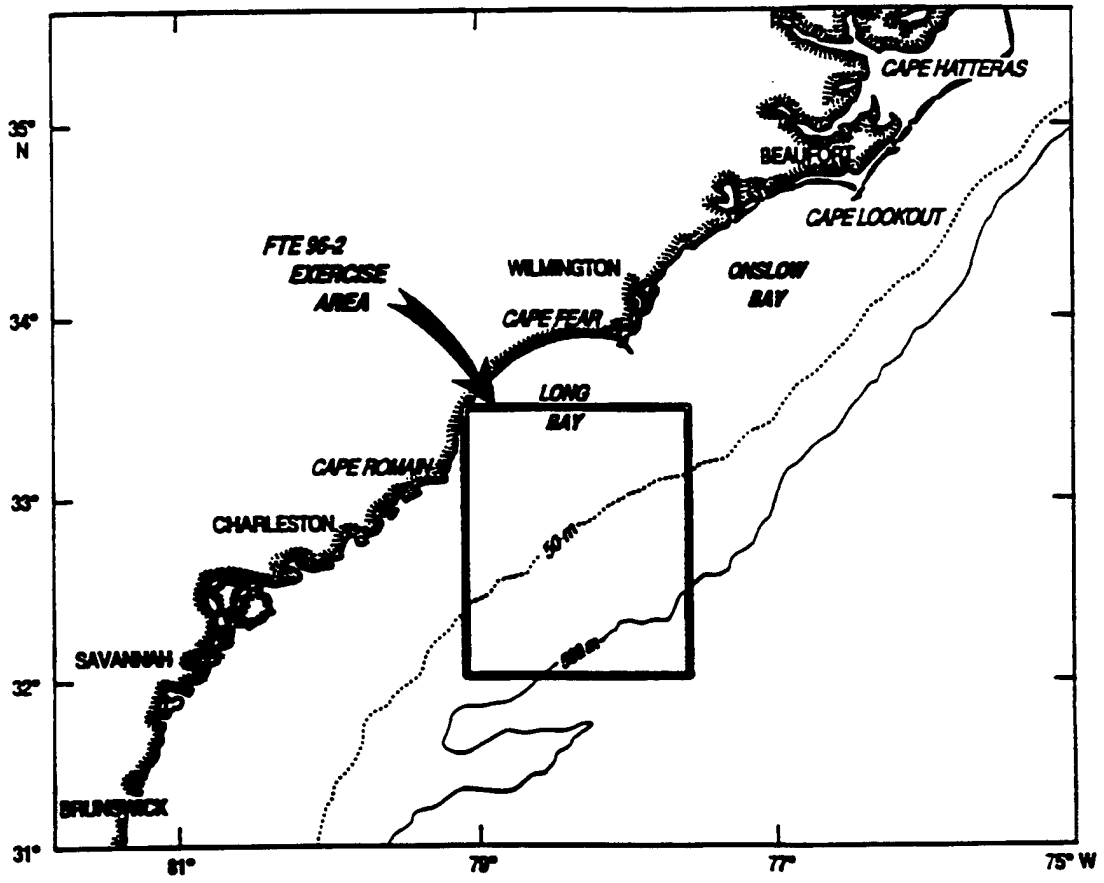


Figure 1: Map of the LWAD FTE 96-2 experiment area.

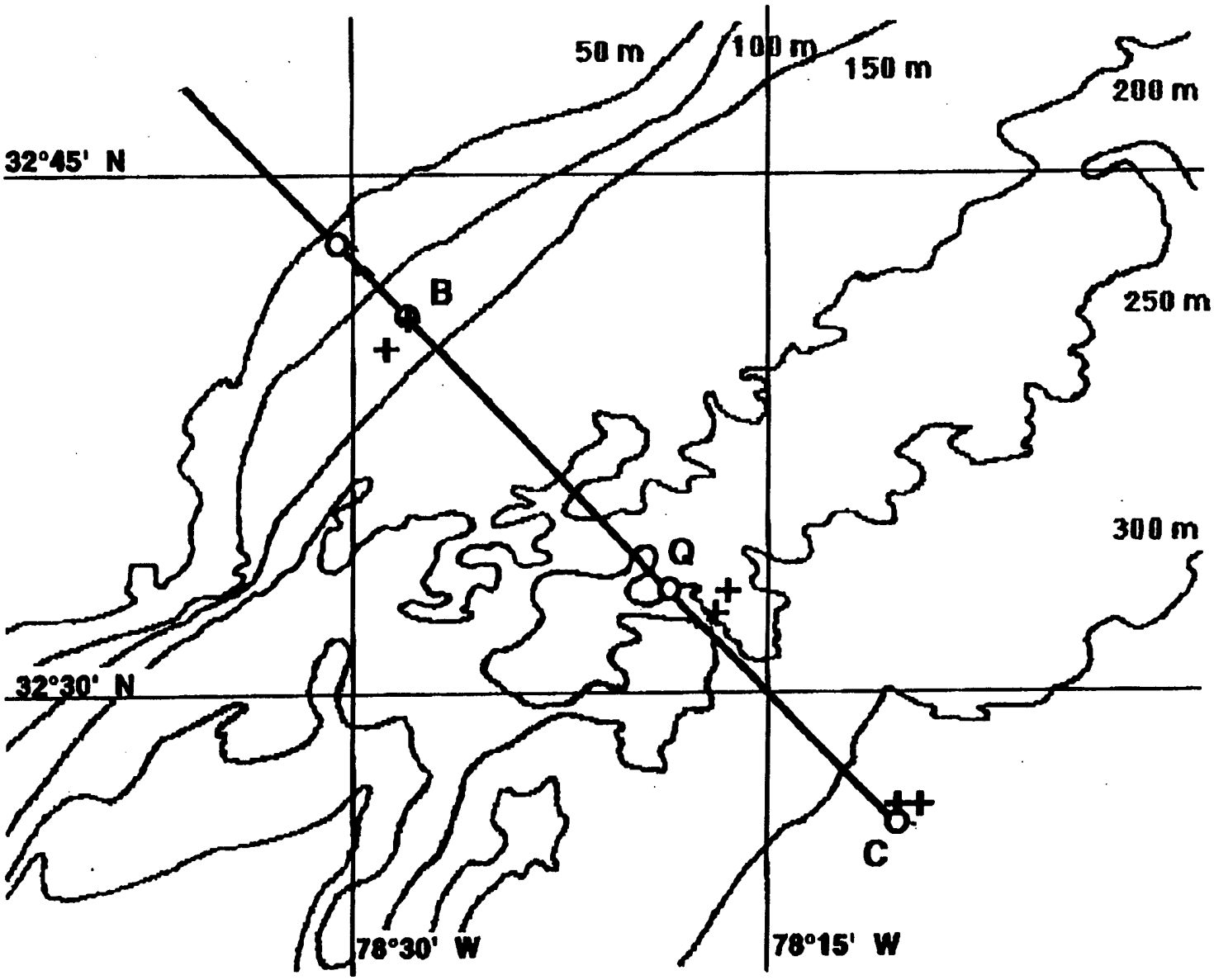


Figure 2: Sites for reverberation measurements during LWAD FTE 96-2. Bottom scattering data were obtained at sites indicated by crossmarks near the planned sites B, Q, and C.

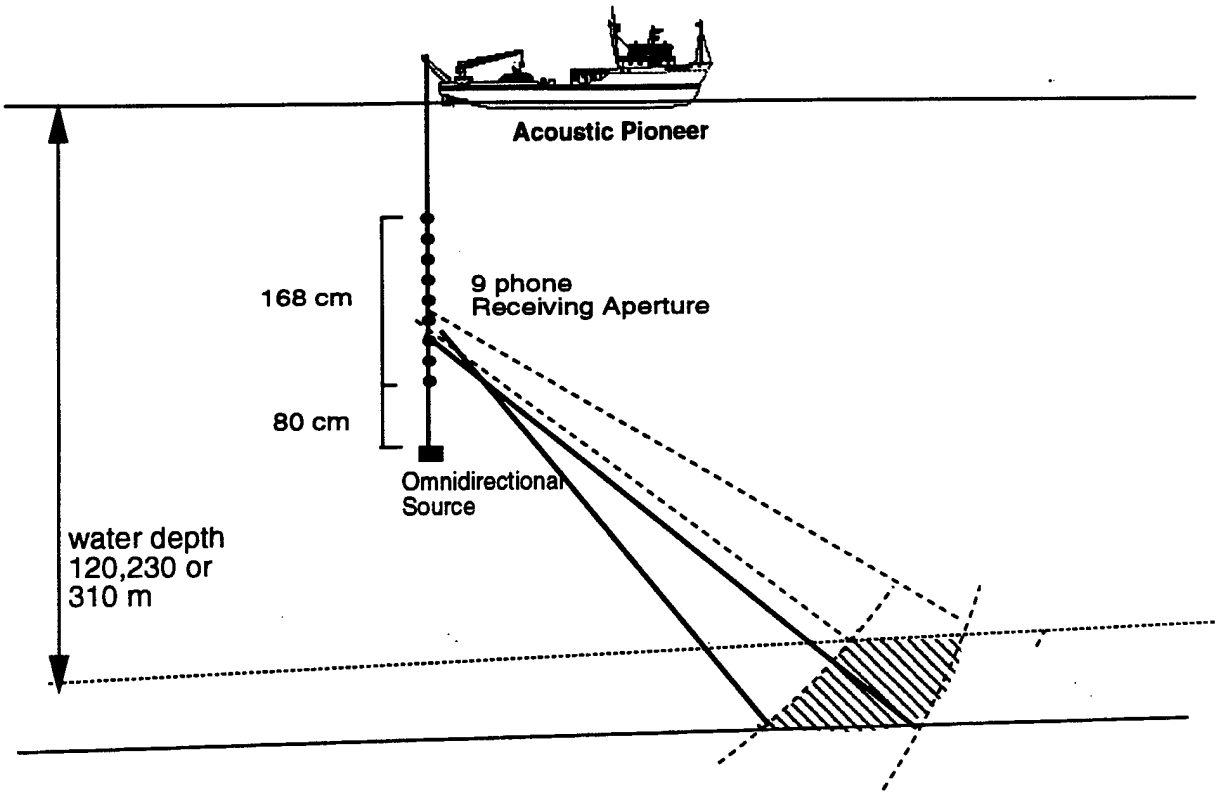


Figure 3: Depiction of the experimental geometry for bottom backscattering measurements in LWAD FTE 96-2. A sector of one receiver beam is shown and a sector of the scattering annulus is shaded.

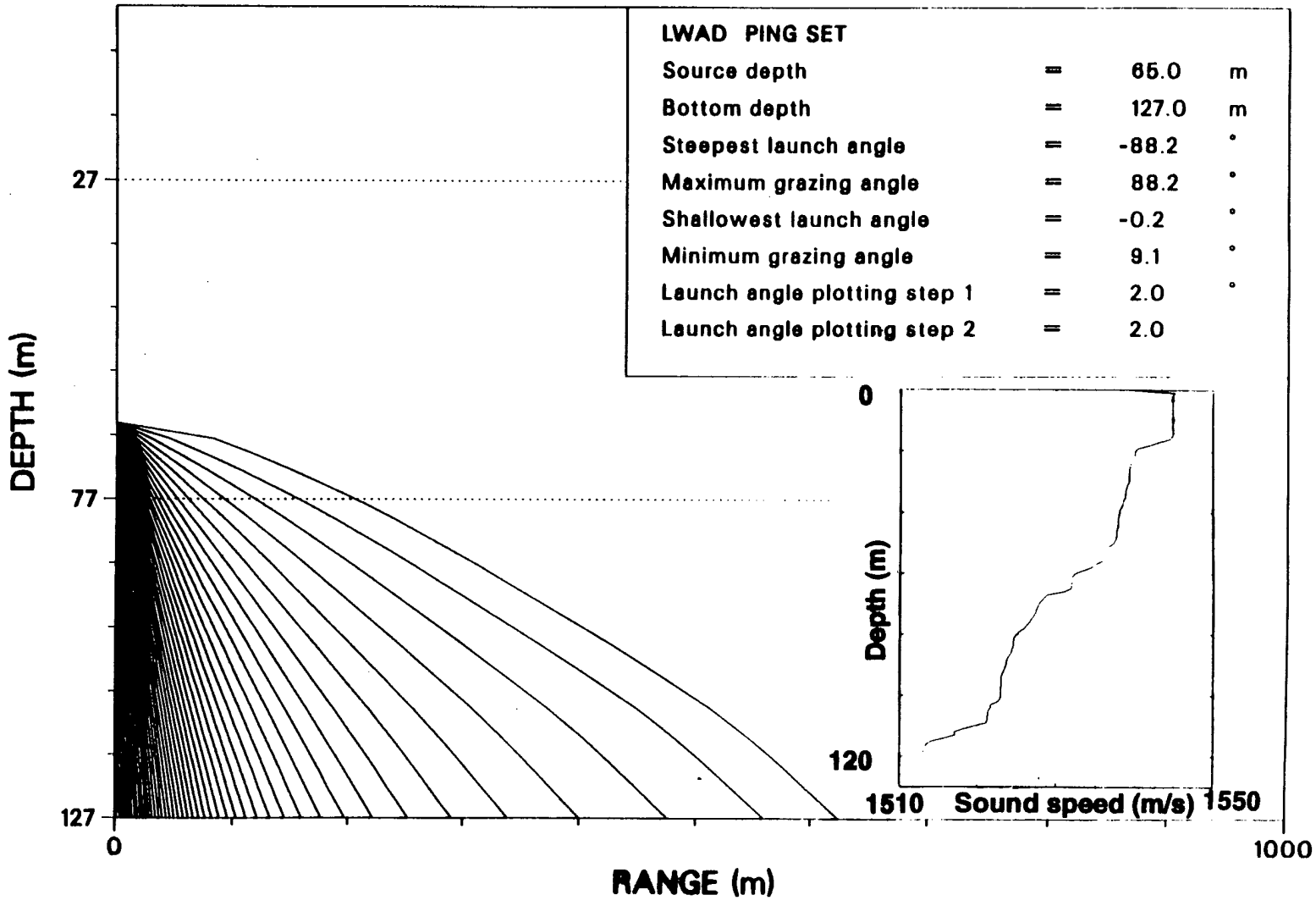


Figure 4: Representative sound speed profile and raytrace for scattering calculations.

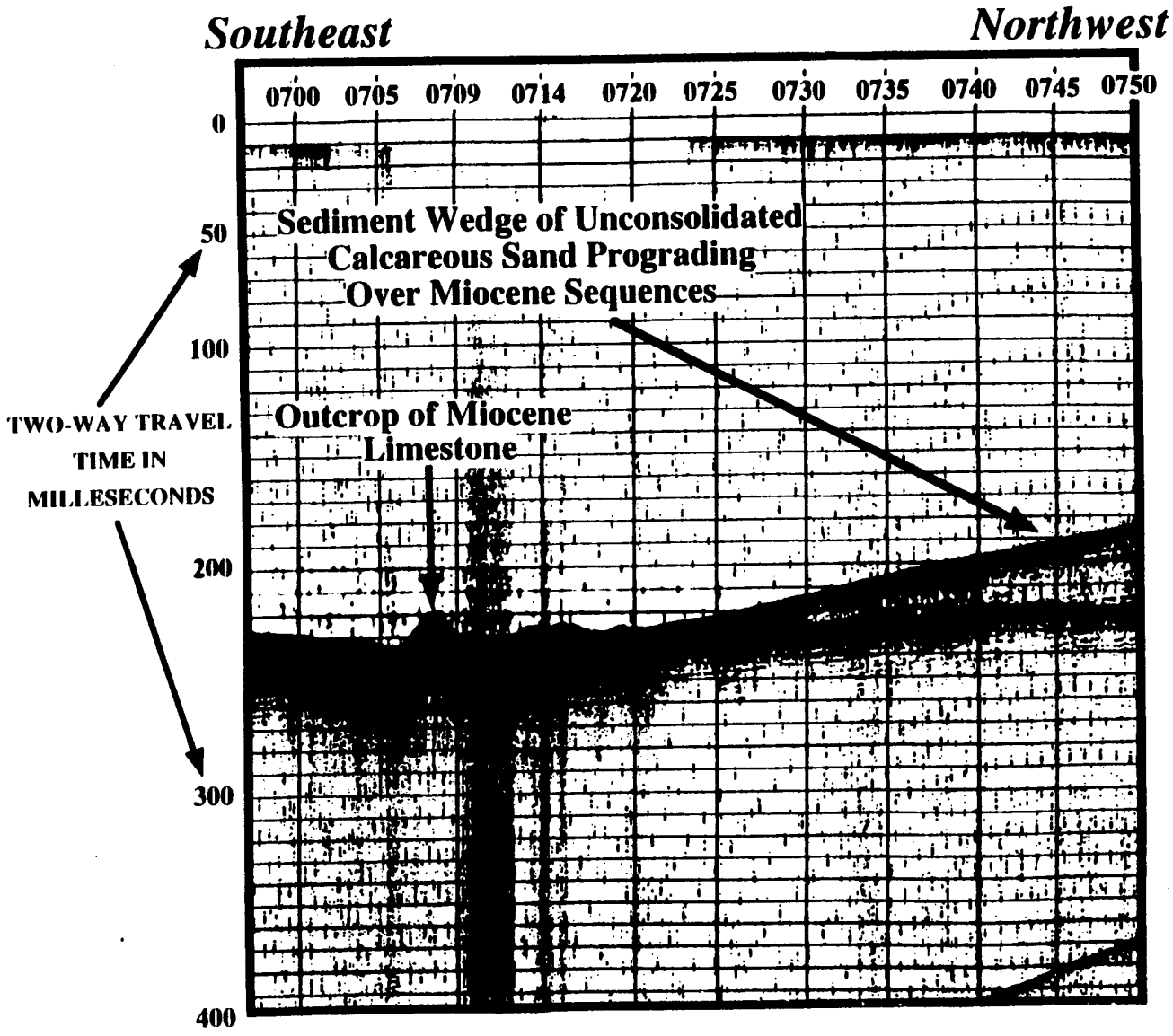


Figure 5: Seismic trace for a track ending in the vicinity of site B (courtesy of Dr. Steve Snyder, North Carolina State University).

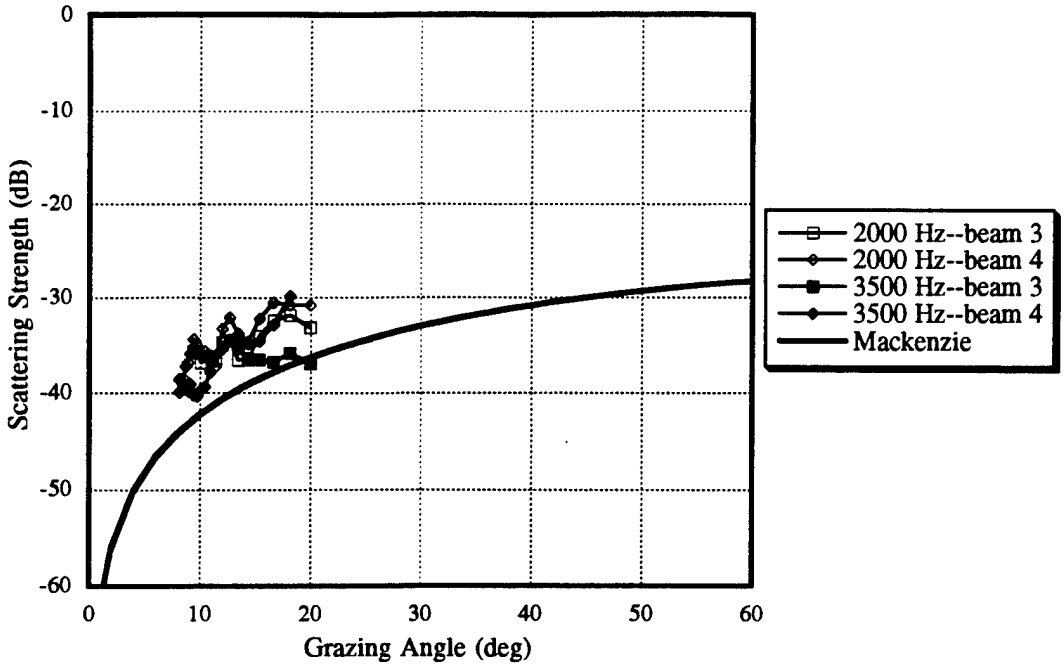


Figure 6: Bottom backscattering strengths as a function of grazing angle for site B with the source deployed at a depth of 60 m.

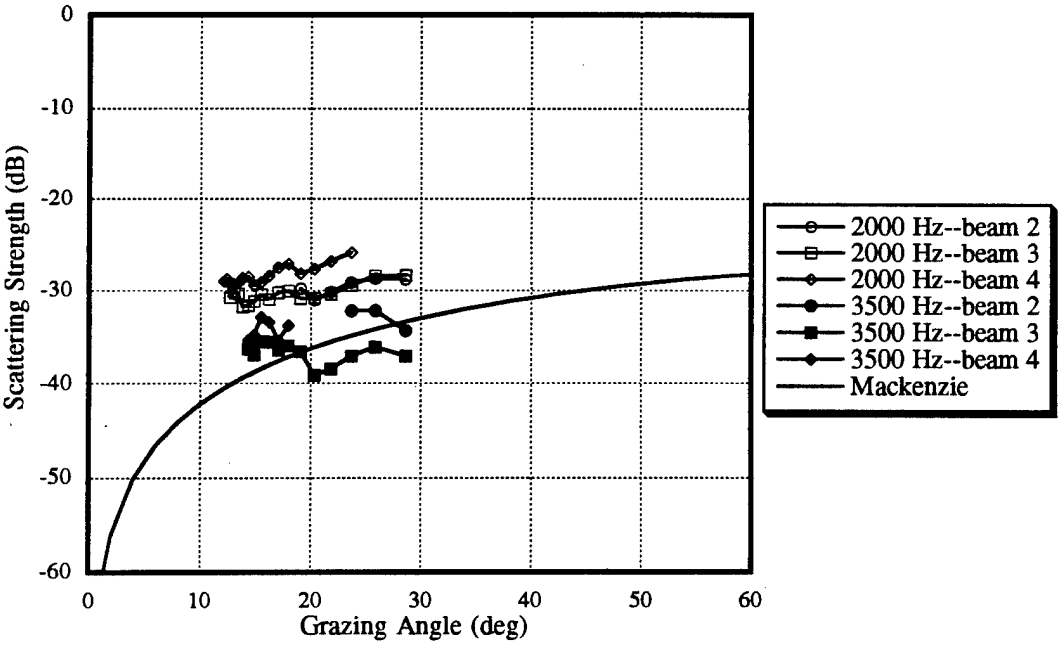


Figure 7: Bottom backscattering strengths as a function of grazing angle for site B with the source deployed at a depth of 35 m.

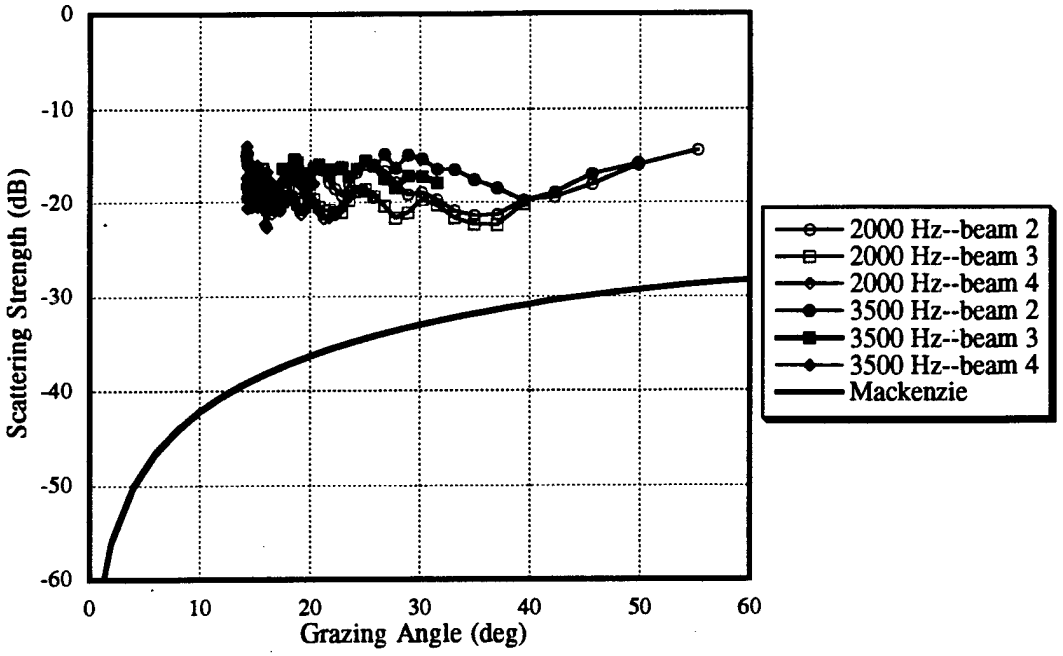


Figure 8: Bottom backscattering strengths as a function of grazing angle for site Q.

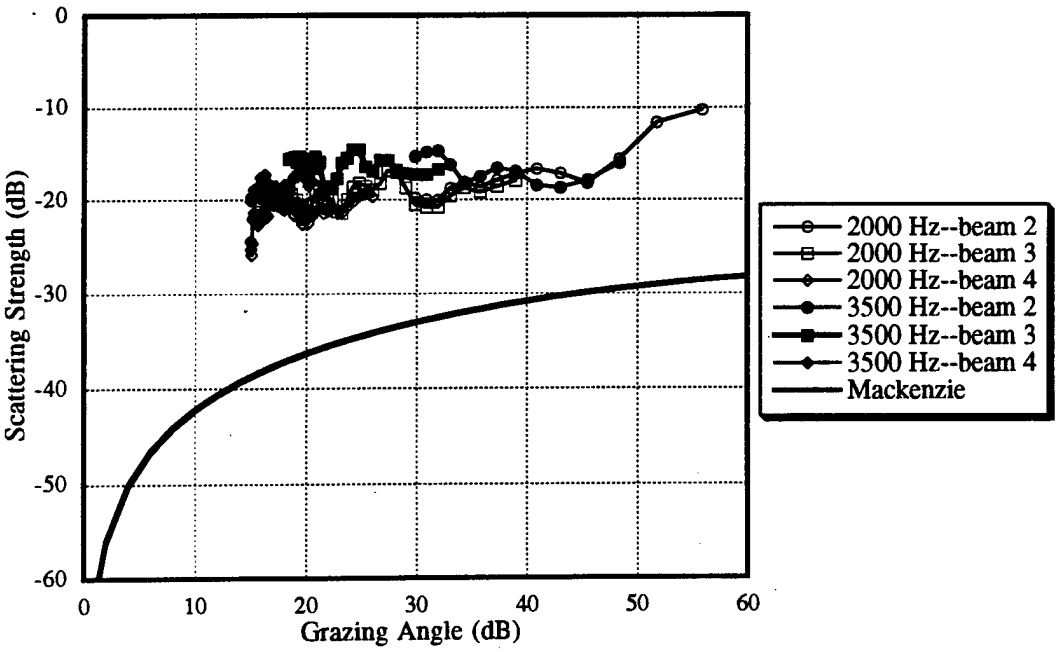


Figure 9: Bottom backscattering strengths as a function of grazing angle for site C.

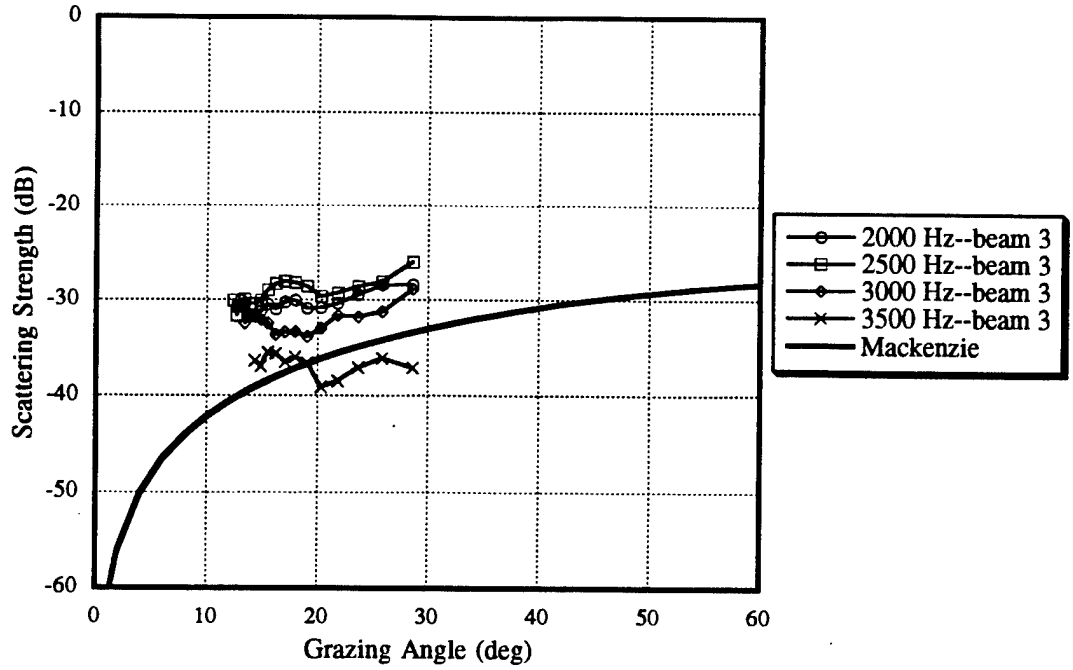


Figure 10: Bottom backscattering strengths as a function of grazing angle for site B at four different frequencies.

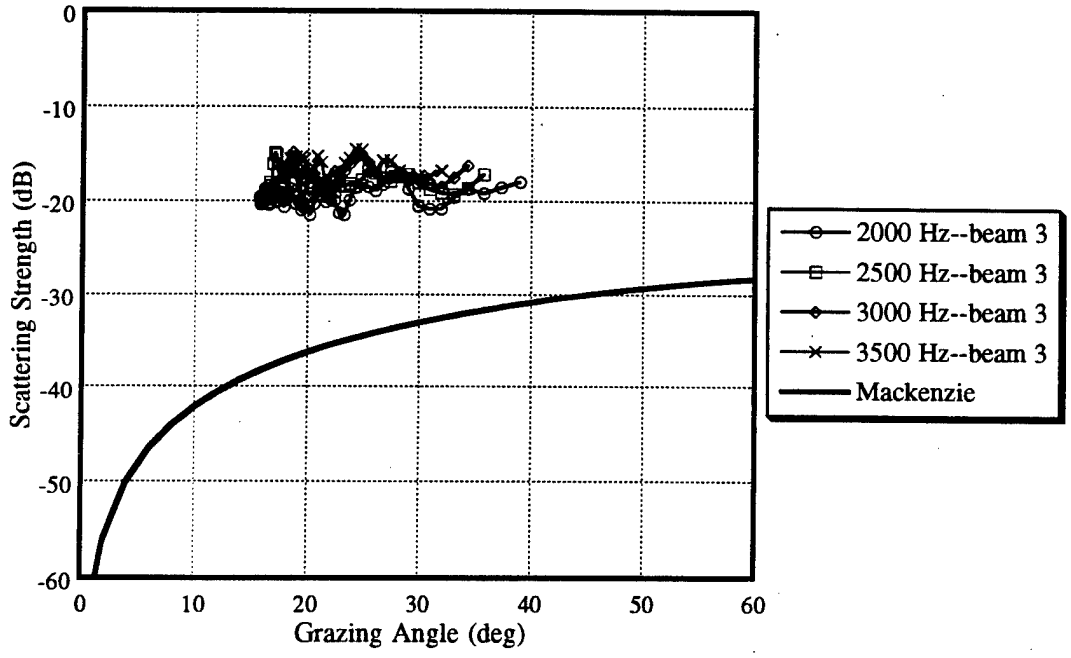


Figure 11: Bottom backscattering strengths as a function of grazing angle for site C at four different frequencies.